

## Atomic structure of Na-adsorbed Si(100) surfaces

Young-Jo Ko and K. J. Chang

*Department of Physics, Korea Advanced Institute of Science and Technology, Taejon 305-338, Korea*

Jae-Yel Yi

*Korea Research Institute of Standards and Science, Taeduk Science-Town, Taejon 305-600, Korea*

(Received 3 October 1994; revised manuscript received 7 November 1994)

We examine the atomic and electronic structure of Na-adsorbed Si(100)- $p(2 \times 2)$  surfaces for various Na coverages ( $\Theta$ ) through first-principles pseudopotential calculations. At  $\Theta = \frac{1}{4}$ , we find that the  $4 \times 1$  structure with linear Na chains adsorbed on the valley bridge sites is energetically most stable, while substrate Si dimers are rearranged by buckling towards the Na chains. At  $\Theta = \frac{1}{2}$ , the adsorption site of Na is the valley bridge site; however, the  $2 \times 2$  structure is found to be more stable than the  $2 \times 1$  structure. From the calculated formation energies, we suggest that the saturation coverage is one monolayer with the Na atoms occupying the pedestal and valley bridge sites, exhibiting a  $2 \times 1$  reconstruction. The coverage dependences of surface geometry and work function are discussed.

### I. INTRODUCTION

The adsorption of alkali metals on semiconductor surfaces has attracted much attention because of its technological and scientific importance. Of special interest are the lowering of the work function, the negative electron affinity state,<sup>1</sup> the metallization mechanism, and Schottky barrier formation of metal-semiconductor interfaces.<sup>2</sup> In this category, alkali-metal adsorption on clean Si(100) surfaces has been intensively studied.<sup>2</sup> However, the adsorption site, the saturation coverage, and the nature of chemical bonds between alkali metal and substrate still remain controversial.<sup>3-20</sup>

The clean Si(100) surface exhibits a  $2 \times 1$  reconstruction, in which the outermost Si atoms are dimerized.<sup>21</sup> It is generally believed that the asymmetric and buckled dimer model [see Fig. 1(a)] is more stable than the symmetric one.<sup>22-27</sup> In the asymmetric dimer model, the up and down atoms of a Si dimer have  $p^3$ - and  $sp^2$ -like bonding configurations, respectively, and a charge transfer from the down atom to the up atom makes the surface free energy lower. However, recent experiments indicated that on the Si(100) surface a correlated buckling of dimers in the form of the  $p(2 \times 2)$  or  $c(4 \times 2)$  structure [see Fig. 1(b) and (c)] is lower in energy than the uncorrelated  $2 \times 1$  structure.<sup>24,28-30</sup>

On the Si(100) surface deposited by Na atoms, the  $2 \times 1$  low energy electron diffraction (LEED) pattern of the clean surface was shown to first change to a  $4 \times 1$  pattern at room temperature, then, a  $2 \times 1$  unit cell is recovered at saturation coverage.<sup>7,9,12,13</sup> At higher temperatures above 500 K, a  $2 \times 3$  structure was observed.<sup>7</sup> As an adsorption site on the Si(100) surface, Levine proposed that adatoms occupy the pedestal sites (denoted as  $HH$  in Fig. 2).<sup>3</sup> Levine's model was supported by dynamical LEED intensity spectra analysis for the Na/Si(100) system.<sup>9</sup> Recently, Mangat and his co-

workers reported a single-adsorption-site model, in which Na atoms are adsorbed on the cave (denoted as  $T4$  in Fig. 2) sites, based on polarization-dependent photoemission extended x-ray-adsorption fine-structure experiments and first-principles cluster calculations.<sup>19</sup> Since the single-site model corresponds to the half-monolayer coverage [one Na atom per Si(100)-( $2 \times 1$ ) unit cell], the alkali-metal adsorbed Si(100) surface is metallic. However, Enta and his co-workers found from their angle resolved photoemission experiments that at the saturation coverage the K/Si(100) system is insulating.<sup>5</sup> Alternatively, Abukawa and Kono proposed a double-layer model,<sup>6</sup> i.e., a one-monolayer-coverage model, in which two sites are adsorbed per Si(100)-( $2 \times 1$ ) unit cell. Recent first-principles total-energy calculations showed that alkali metals occupy the  $HH$  and valley bridge (denoted as  $T3$  in Fig. 2) sites, supporting the double-layer model.<sup>17,18</sup> Experiments such as reflection high energy electron diffraction analysis,<sup>11</sup> inverse photoemission spectroscopy,<sup>12</sup> and medium energy ion scattering<sup>20</sup> also supported the double-layer model. Alkali-metal adsorption induces a significant lowering of the work function, and this behavior was attributed to the dipole layers formed by the ionization of adatoms.<sup>4,14</sup> However, Ishida and Terakura analyzed the nature of the alkali-metal-Si bond and claimed the polarized covalent bond picture even at low coverage.<sup>15</sup>

In this paper we study the atomic and electronic structure of clean and Na adsorbed Si(100) surfaces with use of a first-principles pseudopotential method. We use the  $p(2 \times 2)$  phase of the clean Si(100) surface with the correlated bucklings within the dimer rows as a substrate unit cell. We investigate the energetics of various adsorption sites and the structural change of the surface at different Na coverages. At quarter-monolayer coverage, we report the first theoretical result of the  $4 \times 1$  stable structure, in which Na atoms are adsorbed at the valley

(a) asymmetric dimer

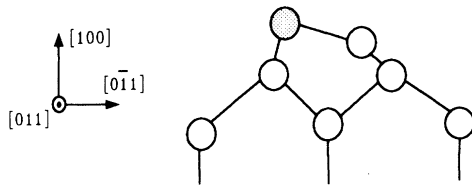
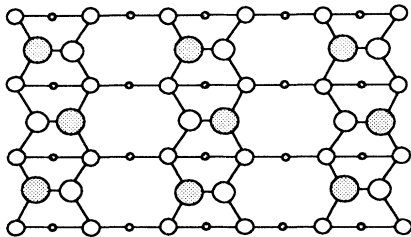
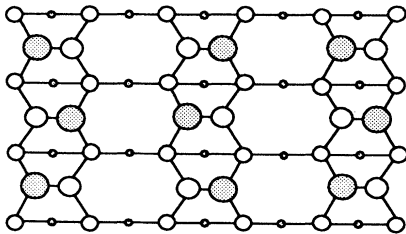
(b)  $p(2 \times 2)$ (c)  $c(4 \times 2)$ 

FIG. 1. (a) A side view of the asymmetric Si dimer and (b), (c) top views of the  $p(2 \times 2)$  and  $c(4 \times 2)$  structures on the clean Si(100) surface. The up atoms of the dimers are denoted by shaded circles.

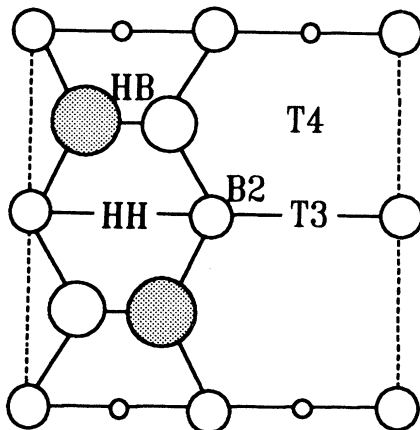


FIG. 2. A top view of the unit cell in the Si(100)- $p(2 \times 2)$  structure. The pedestal, valley bridge, cave, interdimer bridge, and dimer bridge sites are denoted by *HH*, *T3*, *T4*, *B2*, and *HB*, respectively.

bridge sites, while missing rows appear between neighboring linear Na chains. In this case, all the substrate Si dimers are found to be oriented toward the Na chains by a rearrangement of bucklings. As Na coverage increases to half-monolayer, additional deposited Na atoms occupy the missing valley bridge sites. Although the bucklings of the Si dimers are much reduced at this coverage, they still preserve the asymmetric arrangement, exhibiting the  $p(2 \times 2)$  structure. However, the difference of the total energies between the  $p(2 \times 2)$  and  $2 \times 1$  structures is found to be extremely small. At one-monolayer coverage, Na atoms occupy the pedestal sites on the dimer rows as well as the valley bridge sites. Then, the substrate Si atoms form symmetric dimers, and the surface structure exhibits a  $2 \times 1$  pattern. From the calculated formation energies, we suggest that the saturation coverage is one-monolayer and Na atoms are positioned at the pedestal and valley bridge sites within a  $2 \times 1$  unit cell. In Sec. II the computational methods are introduced. The results of our calculations for clean and Na adsorbed Si(100) surfaces are presented in Sec. III. The coverage dependences of the surface structure and the work function are also given. Finally, we summarize the paper in Sec. IV.

## II. METHOD OF CALCULATION

Our calculations are based on an accurate and efficient *ab initio* pseudopotential method within the local-density functional approximation,<sup>31</sup> which allows for the calculations of forces on atoms to relax atomic configurations. The Wigner interpolation formula is used for the exchange and correlation potential.<sup>32</sup> Norm-conserving soft pseudopotentials are generated by the scheme of Troullier and Martins,<sup>33</sup> then, they are transformed into the separable form of Kleinman and Bylander.<sup>34</sup> We include the partial core corrections developed by Louie, Froyen, and Cohen<sup>35</sup> for the Na potential. With the core corrections, the equilibrium lattice constant and the bulk modulus for Na in the bcc structure are calculated to be 4.112 Å and 0.084 Mbar, respectively, while the corresponding measured values are 4.225 Å and 0.068 Mbar.<sup>36</sup> However, neglecting the core corrections, we estimate a much smaller lattice constant of 3.991 Å. The Kohn-Sham equation<sup>31</sup> is solved self-consistently in momentum space using the modified Jacobi relaxation method which was recently developed and employed successfully for a variety of systems.<sup>37</sup> A plane wave basis set is used to expand the wave functions with a kinetic energy cutoff of 10 Ry. To obtain the minimum energy configuration for each surface structure, the Hellmann-Feynman forces<sup>38</sup> are calculated and used for relaxing the ions via the conjugate gradient method until the forces are less than  $3.0 \times 10^{-3}$  Ry/ $a_B$ , where  $a_B$  is the Bohr radius. To perform the Brillouin zone (BZ) integration of the charge density, eight  $\mathbf{k}$  points in the irreducible sector of the BZ are employed for the asymmetric clean Si(100)- $(2 \times 1)$  structure and equivalent  $\mathbf{k}$ -points sets are used for other  $2 \times 2$  and  $4 \times 1$  surface structures.

Surfaces are modeled by a repeated slab geometry. The

Si substrate consists of 10 Si(100) layers and a vacuum region with a thickness of 8 Si layers is inserted between Si slabs. On the clean Si(100) surface, we examine the energetics of the  $2 \times 1$ ,  $p(2 \times 2)$ , and  $c(4 \times 2)$  unit cells. For the Na adsorption on the Si(100) surface, Na atoms are adsorbed on both sides of the Si surfaces. We choose the  $p(2 \times 2)$  unit cell as a starting configuration for the substrate. All the Si atoms except for two Si layers centered in the bulk region are fully relaxed until the optimized configuration is obtained. We investigate most of the plausible adsorption sites for quarter-, half-, and one-monolayer Na coverage models, which have half, one, and two Na atoms in the  $2 \times 1$  unit cell, respectively.

### III. RESULTS AND DISCUSSION

#### A. Clean Si(100) surface

We first examine the optimized geometry of the clean Si(100) surface. In a  $2 \times 1$  unit cell, the asymmetric dimer configuration is found to be energetically more stable by 0.15 eV/dimer than the symmetric dimer model, in good agreement with previous calculations.<sup>30,41</sup> In the asymmetric dimer model, the dimer-bond length is 2.29 Å and this value is smaller than the measured value of 2.46 Å.<sup>39</sup> The difference of the heights between the up and down atoms of a Si dimer is 0.65 Å, which is close to the previously calculated value of 0.54 Å,<sup>17</sup> giving a buckling angle of 16°.

In the  $p(2 \times 2)$  and  $c(4 \times 2)$  structures, the dimers are buckled alternately along each dimer row direction as shown in Fig. 1, while they are arranged in the same direction in the  $2 \times 1$  structure. The neighboring dimer rows in the  $p(2 \times 2)$  structure are buckled in phase while the  $c(4 \times 2)$  structure has the buckling of out of phase. The ordering of the asymmetric dimers in the  $p(2 \times 2)$  and  $c(4 \times 2)$  structures can be understood by considering surface strain energy<sup>40,41</sup> and electrostatic energy gain<sup>42</sup> due to the *antiferromagnetic* arrangement of dimers. Because of the charge transfer between the Si atoms of the asymmetric dimer, each dimer acts as a dipole moment. The antiferromagnetic ordering of the dipole moments within each dimer row was shown to be stabilized through dipole-dipole interactions.<sup>42</sup> Since dimerization is accompanied with large surface relaxations, strains are inevitably accommodated in the near-surface region. However, the relaxations of the sublayer in the  $c(4 \times 2)$  and  $p(2 \times 2)$  structures are found to reduce very effectively the strain energy, as illustrated in Fig. 1. In these ordered structures, the sublayer atoms bonded to the neighboring up Si atoms of the dimers are relaxed toward the up atoms. The subsequent outward relaxations of the sublayer atoms bonded to the down Si atoms reduce the heights of the down atoms, thus, the amount of buckling is slightly increased. We find the displacements of the sublayer atoms from their positions in the  $2 \times 1$  structure to be about 0.1 Å along the dimer row direction. Similar relaxations were also found on Ge(100) surfaces.<sup>43</sup>

We find that the  $p(2 \times 2)$  and  $c(4 \times 2)$  structures are more stable by 0.1 eV/dimer than for the asymmetric

$2 \times 1$  structure, in good agreement with other theoretical calculations.<sup>30,40,41</sup> However, the energies of these ordered structures are nearly the same because the interactions between neighboring dimer rows are negligible. The dimer-bond length in the  $p(2 \times 2)$  structure is estimated to be 2.36 Å, which is slightly larger than that of the asymmetric  $2 \times 1$  structure, thus, it is closer to the measured value.<sup>39</sup> The vertical distance between the up and down atoms of a dimer is 0.72 Å, giving an increased buckling angle of 17.8°, as compared to the asymmetric dimer model. Similar results for the dimer-bond length and the buckling of the asymmetric dimer are found in the  $c(4 \times 2)$  structure.

#### B. Na-adsorbed Si(100) surfaces

To find plausible adsorption sites of Na on the Si(100) surface, the  $p(2 \times 2)$  structure is chosen as a starting configuration for the substrate, while previous work<sup>17,18</sup> used the asymmetric  $2 \times 1$  structure. Thus, we examine the effect of the ordering of the Si dimers on the optimized geometry of Na/Si(100) systems. The adsorption sites of Na are determined by calculating the adsorption energy ( $E_{ad}$ ) per Na on the Si(100) surface, which is defined as;

$$E_{ad} = (E_{Si} + nE_{Na}^a - E_{Si+Na})/n, \quad (1)$$

where  $E_{Si}$  and  $E_{Si+Na}$  are the total energies of the clean and Na adsorbed Si(100) surfaces, respectively.  $E_{Na}^a$  is the total energy of a spin-polarized free Na atom and  $n$  denotes the number of adsorbed Na atoms. If the Na coverage ( $\Theta$ ) is defined as the ratio of the number of Na atoms to that of the outermost Si atoms,  $\Theta = \frac{1}{4}$ ,  $\Theta = \frac{1}{2}$ , and  $\Theta=1$  correspond to 0.5, 1, and 2 adatoms per Si dimer, respectively.

At  $\Theta = \frac{1}{4}$ , we consider two ordered structures in the  $2 \times 2$  and  $4 \times 1$  units. The adsorption energies calculated for high symmetry adsorption sites such as *B2*, *HH*, *T3*, and *T4* in Fig. 2 are listed in Table I for both the  $2 \times 2$  and  $4 \times 1$  structures. We find that the *T3* site in the  $4 \times 1$  unit cell has the highest adsorption energy, indicating that the  $4 \times 1$  structure is the stable geometry at  $\Theta = \frac{1}{4}$ . This

TABLE I. Adsorption energies ( $E_{ad}$  in eV) at various sites denoted in Fig. 2 are compared at  $\frac{1}{4}$ -,  $\frac{1}{2}$ -, and 1-monolayer coverages.

$\Theta$	Adsorption sites	$E_{ad}$		
		$(2 \times 1)$	$(2 \times 2)$	$(4 \times 1)$
$\frac{1}{4}$	<i>T3</i>		1.94	2.22
	<i>T4</i>		1.98	1.99
	<i>HH</i>		1.95	1.97
	<i>B2</i>		1.50	1.78
$\frac{1}{2}$	<i>T3-T3</i>		1.94	
	<i>T4-T4</i>		1.84	
	<i>HH-HH</i>		1.76	
1	<i>T3-HH</i>	2.06		
	<i>T4-HH</i>	1.99		

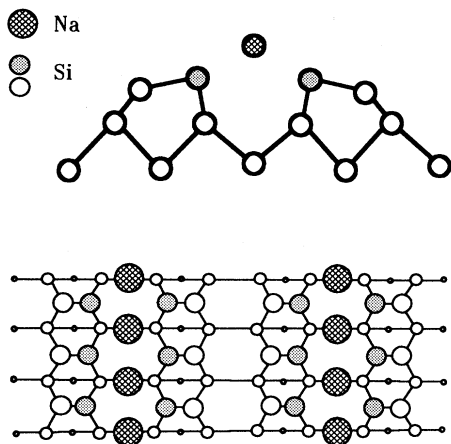


FIG. 3. Side and top views of the optimized geometry of the  $4 \times 1$  structure at  $\Theta = \frac{1}{4}$ , in which Na occupies the  $T3$  site.

result is in good agreement with LEED experiments that frequently showed the  $4 \times 1$  pattern at low Na coverages near  $\Theta = \frac{1}{4}$ .<sup>7,9,12,13</sup> The  $T4$  site is less stable by 0.23 eV per Na atom than for the  $T3$  site, while this site is most stable in the  $2 \times 2$  structure. Among the adsorption sites considered here, the adsorption energy is found to be smallest at the  $B2$  site in both the  $4 \times 1$  and  $2 \times 2$  structures.

The optimized geometry for the  $T3$  adsorption in the  $4 \times 1$  unit cell is shown in Fig. 3, and the Si-Si and Na-Si bond distances are listed in Table II. The  $4 \times 1$  periodicity is simply constructed by forming linear Na chains along the dimer row direction, accompanied with missing rows between Na chains. Thus, the separation between the neighboring Na chains is twice larger than the distance of 7.68 Å between the dimer rows. At the  $T3$  site, the Na atom is bonded more closely to the second layer Si atoms with the bond length of 3.16 Å, while the separation between Na and the up atom of the asymmetric dimer is 3.20 Å. As compared to the clean Si(100) surface, the dimer-bond length of 2.39 Å is slightly increased, however, the amount of buckling of the asymmetric dimer is significantly reduced to 0.37 Å.

As Na atoms occupy the  $T3$  sites, all the asymmetric dimers are oriented towards the Na chains as shown in Fig. 3, whereas in the  $2 \times 2$  structure a correlated buckling of the dimers is retained, similar to the clean  $p(2 \times 2)$

structure. On the clean Si(100) surface, the asymmetric dimers are correlated along the dimer row direction, i.e., the nearby dimers within a dimer row are buckled in opposite directions (see Fig. 1). In the  $2 \times 2$  structure at  $\Theta = \frac{1}{4}$ , since only one  $T4$  site in the unit cell is occupied along the dimer row direction, the Na atoms more strongly affect the dimer-bond length and the degree of buckling of the neighboring dimers. However, the asymmetric dimers are arranged in the same way as that on the clean Si(100) surface. For the dimer adjacent to the Na atom, the dimer-bond length and the difference in height of the dimer Si atoms are 2.43 and 0.28 Å, respectively, while the corresponding values are 2.32 and 0.53 Å for the other dimer. However, in the  $4 \times 1$  structure, the bucklings of the asymmetric dimers are closely related to the adsorption site of Na and the ionized Na potential, because the Na chains are well separated by a missing row. When an asymmetric dimer is formed, it is known that more electron charges are accumulated at the up Si atom than at the down atom because of the charge transfer between the two atoms. Since the Na atom is slightly ionized upon adsorption, it is likely to be positioned near the up atom of the asymmetric dimer. If the up atoms of the dimers are rearranged towards the adjacent Na chain, the  $T3$  site is ideally fitted to the adsorption site because this site is surrounded by more up atoms than for the  $T4$  site, resulting in more attractive interactions.

The clean  $p(2 \times 2)$  surface gives an equal number of filled ( $S_{1,2}$ ) and empty ( $S_{1,2}^*$ ) surface states in the gap region, which are originated from the dangling bonds of the up and down atoms, respectively, of the asymmetric dimer. The filled  $S_{1,2}$  bands exhibit a large pileup of charge densities around the up atom. At  $\Theta = \frac{1}{4}$ , the unoccupied  $S_{1,2}^*$  bands of the clean Si(100) surface are partially filled by Na electrons. For Na at the  $T3$  site in the  $4 \times 1$  cell, the electron charge densities for the newly occupied state are plotted in Fig. 4(a). We find that the charge densities of the newly occupied state are mostly accumulated near the down atom of the dimer. The occupation of the  $S_{1,2}^*$  bands by the electrons of ionized adatoms was often regarded as evidence of the ionic nature of the alkali-metal-Si bond. However, from the analysis of the surface bands, it was suggested that the polarized covalent bond picture is more appropriate.<sup>15,17</sup> We find no directional bonding between the Na and Si atoms and attribute the reduction of buckling of the asymmetric dimer to the charge transfer from Na to the Si dangling bonds. The charge densities for the surface states in Fig.

TABLE II. Calculated Si-Si ( $d_{\text{Si-Si}}$ ) and Na-Si ( $d_{\text{Na-Si}}$ ) bond distances (in units of Å) are given in the optimized geometries of the most stable structures at various Na coverages. The amount of buckling of the Si-Si dimer is given in parentheses. Si(1) and Si(2) represent the Si atoms in the first and second layers, respectively. The Na adsorption sites are denoted by  $T3$  and  $HH$  in Fig. 2.

$\Theta$	Structure	$d_{\text{Si-Si}}$	$d_{\text{Na-Si}}$		
			Na( $T3$ )-Si(1)	Na( $T3$ )-Si(2)	Na( $HH$ )-Si(1)
0	$2 \times 2$	2.36 (0.65)			
$\frac{1}{4}$	$4 \times 1$	2.39 (0.37)	3.20	3.16	
$\frac{1}{2}$	$2 \times 2$	2.46 (0.12)	3.35, 3.46	3.10	
1	$2 \times 1$	2.63 (0.00)	3.30	3.07	2.96

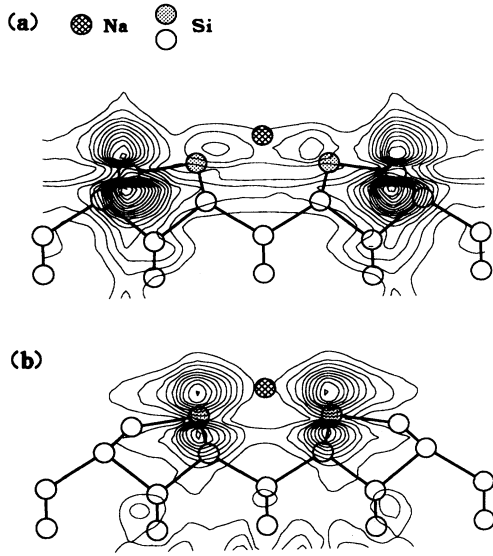


FIG. 4. The charge density contours for the (a)  $S_{1,2}^*$  and (b)  $S_{1,2}$  states in the  $4 \times 1$  structure at  $\Theta = \frac{1}{4}$  are plotted on the planes containing the Si dimers. The Na atom is adsorbed at the  $T3$  site.

4 exhibit  $p_z$ -like orbitals, very similar to those for the Si dangling bond states of the clean Si(100) surface. Thus, the weak covalency is preserved between the Na and surface Si atoms. For both the  $T3$ - and  $T4$ -site adsorptions in the  $4 \times 1$  unit cell, the energy separation between the  $S_{1,2}$  and  $S_{1,2}^*$  bands is found to be about 1.0 eV, with a band width of 0.8 eV for each band. However, for the  $T4$ -site adsorption in the  $2 \times 2$  structure, this energy separation is much reduced, giving rise to a slight overlap between the  $S_{1,2}$  and  $S_{1,2}^*$  bands.

At  $\Theta = \frac{1}{2}$ , we only consider the  $2 \times 2$  unit cell, in which two Na atoms occupy two equivalent sites. Although our calculations are similar to previous work<sup>14,17,18</sup> using the  $2 \times 1$  unit cell, the use of the  $2 \times 2$  unit cell can treat more effectively the correlation of the asymmetric dimers. The calculated adsorption energies at the  $T3$ - $T3$ ,  $T4$ - $T4$ , and  $HH$ - $HH$  sites are listed in Table I. The adsorption energy is found to be largest at the  $T3$ - $T3$  sites. In this case, since the Na atoms occupy all the  $T3$  sites between the dimer rows, the Na potentials do not change the correlated bucklings of the substrate dimers. Thus, the optimized geometry of the minimum energy state exhibits the same  $p(2 \times 2)$  periodicity as that of the clean surface. At the  $T3$  site, the Na atom is more closely bonded to the second-layer Si atoms with the bond distance of 3.10 Å than to the dimer atoms as shown in Table II. The Na-Si bond distances are found to be 3.35 and 3.46 Å for the up and down atoms, respectively, of the dimer. In the  $2 \times 2$  structure, the dimer-bond length is increased to 2.46 Å, compared with the stable  $4 \times 1$  structure at  $\Theta = \frac{1}{4}$ , while the amount of buckling of the asymmetric dimer is significantly reduced to 0.12 Å, close to the symmetric dimer. However, this amount of buckling is much larger than the results of Kobayashi and his co-

workers,<sup>17</sup> who reported 0.01 Å for the very weak  $p(2 \times 2)$  structure. Such a discrepancy may result from the use of smaller plane waves, because the use of an insufficient basis set was shown to lead to a more symmetric dimer configuration;<sup>41</sup> a smaller kinetic energy cutoff of 6.25 Ry was employed in their calculations. When we test the  $2 \times 1$  geometry with the symmetric dimers, the energy is only increased by 0.007 eV per  $2 \times 1$  unit cell. Thus, our results for the Na-adsorption sites basically agree with recent pseudopotential calculations that used the  $2 \times 1$  unit cell.<sup>17,18</sup> Although the  $HH$  site was reported in an earlier pseudopotential work,<sup>14</sup> more accurate calculations using a larger plane wave basis showed the  $T3$  site.<sup>18</sup> Recently, it was shown that the stable site is changed from the  $T4$  site to the  $T3$  site when the partial core corrections are included for the Na potentials.<sup>17</sup> In contrast, other cluster calculations showed that the adsorption sites are the  $T4$  sites.<sup>19</sup> However, these calculations did not fully take into account the Na chain structure because of the small size of the clusters.

At  $\Theta = 1$ , we test various adsorption sites and find the  $T3$ - $HH$  sites to be lowest in energy. The adsorption energy at the  $T3$ - $HH$  sites is higher by 0.13 eV per  $2 \times 1$  unit cell than that for the  $T4$ - $HH$  sites, which is consistent with previous calculations.<sup>17,18</sup> At this Na coverage, the adsorption energy is larger by 0.12 eV than that calculated at  $\Theta = \frac{1}{2}$ . The bond distances in the optimized geometry of the lowest energy state are given and compared in Table II. The asymmetric dimers are completely changed to the symmetric ones with the bond length of 2.63 Å. Thus, the surface structure exhibits the  $2 \times 1$  periodicity. The bond distances between the Na and its nearest neighbor Si atoms are calculated to be 2.96 and 3.07 Å at the  $HH$  and  $T3$  adsorption sites, respectively, and these values are in good agreement with other calculations.<sup>17,18</sup> Since the surface bands are fully occupied, the  $2 \times 1$  structure is insulating at one-monolayer Na coverage.<sup>14,17,18</sup>

### C. Coverage dependences of structure and work function

If a Na-adsorbed Si surface is in equilibrium with the Na reservoir, the surface formation energy ( $\Omega_f$ ) is written as a function of the Na chemical potential ( $\mu_{\text{Na}}$ ),<sup>44</sup>

$$\Omega_f = E_{\text{Si+Na}} - m\mu_{\text{Si}} - n\mu_{\text{Na}}, \quad (2)$$

where  $\mu_{\text{Si}}$  is the total energy of bulk Si and  $n$  denotes the average number of Na atoms adsorbed on the  $1 \times 1$  unit area. In usual deposition experiments using a gaseous Na,  $\mu_{\text{Na}}$  is smaller than its bulk value, and it varies with temperature and pressure.<sup>45</sup>

The calculated formation energies are plotted as a function of  $\mu_{\text{Na}}$  in Fig. 5. The bulk energy for  $\mu_{\text{Na}}$  is chosen as the origin of the chemical potential. For  $\mu_{\text{Na}} < -1.14$  eV, the clean  $p(2 \times 2)$  structure is a stable form of the surface. As  $\mu_{\text{Na}}$  increases to  $-0.91$  eV, the surface structure changes to the  $4 \times 1$  structure at  $\Theta = \frac{1}{4}$ . With the further increase of  $\mu_{\text{Na}}$  to its maximum value, the

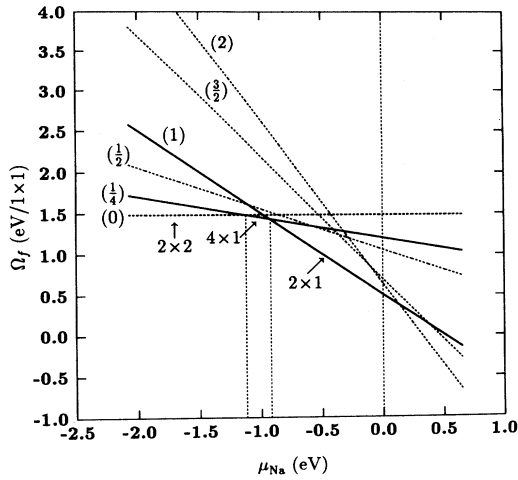


FIG. 5. The formation energies are plotted as a function of the Na chemical potential for each stable structure at coverages  $\Theta = \frac{1}{4}$ ,  $\frac{1}{2}$ , 1,  $\frac{3}{2}$ , and 2. The bulk value for  $\mu_{\text{Na}}$  is taken as the origin. The most stable structure is marked by arrows as  $\mu_{\text{Na}}$  increases.

stable structure becomes the  $2 \times 1$  phase at  $\Theta = 1$ . It is interesting to note that the  $2 \times 1$  or  $2 \times 2$  structure at  $\Theta = \frac{1}{2}$  cannot be stable over the whole range of  $\mu_{\text{Na}}$  because its formation energy is always higher than those at  $\Theta = \frac{1}{4}$  and 1. We also calculate the formation energies at  $\Theta = \frac{1}{2}$  and  $\Theta = 2$ , and find that a uniform coverage of Na over one monolayer is thermodynamically unstable. Based on the calculated formation energies, we suggest that the saturation coverage is one-monolayer.

Using the  $2 \times 2$  unit cell, we examine the migration of a Na atom over the Si surface, and the energy barriers are plotted in Fig. 6. We choose two different diffusion paths that go through low energy sites. For each position of Na, the total energy is fully optimized by relaxing the Si atoms and the height of the Na atom. We find an extremely small barrier height of 0.04 eV along the  $T4-T3-T4$  path, while the energy barrier is 0.15 eV along the  $HH-B2-T3-B2-HH$  path. Thus, we expect that Na on the Si surface diffuses very easily at room temperature. As discussed earlier, because at low Na coverage the  $4 \times 1$  phase at  $\Theta = \frac{1}{4}$  has a lower formation energy

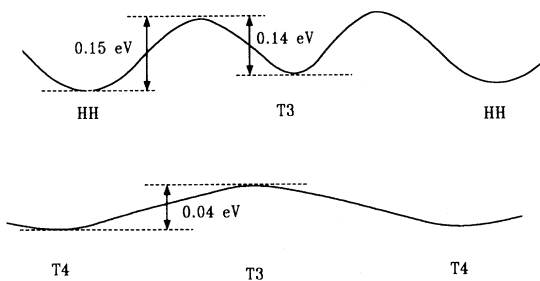


FIG. 6. Energy barriers for the surface diffusion of Na on the clean Si(100) surface.

than other structures calculated at  $\Theta = \frac{1}{2}$  and 1, the Si surface will be initiated by the  $4 \times 1$  phase. As more Na atoms are added, since the formation energy at  $\Theta = 1$  is lower than that for  $\Theta = \frac{1}{2}$ , additional deposited Na atoms may not be uniformly distributed over the surface, but they may coalesce to form locally the  $2 \times 1$  phase of  $\Theta = 1$  coverage. Then, the surface would be composed of a mixture of the  $4 \times 1$  and  $2 \times 1$  phases. With further depositions, the surface then changes to the  $2 \times 1$  structure at  $\Theta = 1$ . For  $\Theta > 1$ , extra Na atoms reside on the Na layer, therefore, the change of the formation energy is mainly affected by the interactions between Na atoms. We find that assuming the uniform deposition over one-monolayer Na adsorbed surface the adsorption energies at  $\Theta = \frac{3}{2}$  and 2 are lower than the cohesive energy of bulk Na. Thus, the layer-by-layer growth mode is not expected, whereas under sufficiently high pressures close to the vapor pressure of Na, three dimensional islands may possibly be formed for coverages over  $\Theta = 1$ . These results lead us to conclude that the saturation coverage is one-monolayer, which agrees well with other theoretical results and experimental observations of strong  $2 \times 1$  LEED patterns and insulating behavior of the surface band at the saturation coverage.<sup>7,12</sup>

The work function ( $\Delta\Phi$ ) is defined as the difference between the vacuum and highest occupied levels. The coverage dependence of the work function is plotted with respect to the clean  $p(2 \times 2)$  structure in Fig. 7, assuming that the surface structure varies with Na coverage. At  $\Theta = \frac{1}{4}$ ,  $\Delta\Phi$  is calculated to be  $-1.4$  eV, which agrees well with the measured value of  $-1.5$  eV.<sup>7,12,13</sup> At  $\Theta = 1$ , we find that  $\Delta\Phi$  is lowered to  $-2.8$  eV, in good agreement with other calculated value of  $-2.7$  eV.<sup>17</sup> Experiments showed that near the saturation coverage the work function is dropped very rapidly to  $-3.0$  eV at room temperature,<sup>7,12,13</sup> while a smooth decrease to  $-2.7$  eV was found for annealed samples.<sup>13</sup>

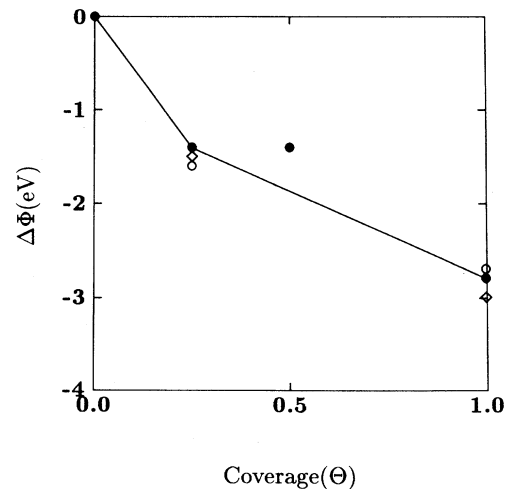


FIG. 7. Coverage dependence of the work function. Filled circles represent calculated values and experimental data are marked by empty circles (Ref. 13) and diamonds (Ref. 12).

#### IV. CONCLUSIONS

We have performed the first-principles pseudopotential calculations for studying the optimized geometry of Na adsorbed Si(100) surfaces. At quarter-monolayer Na coverage, the most stable surface structure is found to be the  $4 \times 1$  structure, in which the linear Na chains are formed by occupying the valley bridge sites together with the missing rows between the Na chains. In this case, the asymmetric dimers are rearranged by buckling towards the Na chains, while the clean surface has the  $p(2 \times 2)$  periodicity with a correlated buckling along the dimer row direction. At half-monolayer coverage, the Na atoms occupy the valley bridge sites in the  $2 \times 2$  unit cell, saturating the missing rows in the  $4 \times 1$  structure at  $\Theta = \frac{1}{4}$  and reducing the degree of buckling. Although the Si dimers exhibit the same  $p(2 \times 2)$  periodicity as the clean surface, the energy difference between the  $2 \times 2$

and  $2 \times 1$  structures is extremely small. At one-monolayer coverage, the pedestal and valley bridge sites are occupied by the Na atoms, and all the asymmetric dimers are changed into the symmetric ones, giving a  $2 \times 1$  relaxation. From the calculated formation energies at different coverages, we suggest that the saturation coverage is one monolayer. Our calculations indicate that the clean Si surface changes to the  $4 \times 1$  structure as Na coverage increases, then, to the  $2 \times 1$  pattern at the saturation coverage. In this case, the  $2 \times 2$  structure at intermediate coverages does not appear because its formation energy is relatively higher.

#### ACKNOWLEDGMENTS

This work was supported by the SPRC at Jeonbuk National University and by the CMS at Korea Advanced Institute of Science and Technology.

- <sup>1</sup> R. U. Martinelli, Appl. Phys. Lett. **16**, 261 (1970).
- <sup>2</sup> *Metallization and Metal/Semiconductor Interfaces*, Vol. 195 of NATO Advanced Study Institute, Series B: Physics, edited by I. P. Batra (Plenum, New York, 1989).
- <sup>3</sup> J. D. Levine, Surf. Sci. **34**, 90 (1973).
- <sup>4</sup> R. W. Gurney, Phys. Rev. **47**, 479 (1935).
- <sup>5</sup> Y. Enta, T. Kinoshita, S. Suzuki, and S. Kono, Phys. Rev. B **36**, 9801 (1987).
- <sup>6</sup> T. Abukawa and S. Kono, Phys. Rev. B **37**, 9097 (1988).
- <sup>7</sup> G. S. Glander and M. B. Webb, Surf. Sci. **222**, 64 (1989); **224**, 66 (1989).
- <sup>8</sup> H. Tochiyama, Surf. Sci. **34**, 90 (1983).
- <sup>9</sup> C. M. Wei, H. Huang, S. Y. Tong, G. S. Glander, and M. B. Webb, Phys. Rev. B **42**, 11 284 (1990).
- <sup>10</sup> T. Hashizume, I. Sumita, Y. Murata, S. Hyodo, and T. Sakurai, J. Vac. Sci. Technol. B **9**, 742 (1991).
- <sup>11</sup> T. Makita, S. Kohmoto, and A. Ichimiya, Surf. Sci. **242**, 65 (1991).
- <sup>12</sup> L. S. O. Johansson and B. Reihl, Phys. Rev. Lett. **67**, 2191 (1991); Phys. Rev. B **47**, 1401 (1993); Surf. Sci. **287/288**, 524 (1993).
- <sup>13</sup> M. Tikhov, G. Boishin, and L. Surnev, Surf. Sci. **241**, 103 (1991).
- <sup>14</sup> I. P. Batra, Phys. Rev. B **43**, 12 322 (1991).
- <sup>15</sup> H. Ishida and K. Terakura, Phys. Rev. B **40**, 11 519 (1989).
- <sup>16</sup> Y. Morikawa, K. Kobayashi, K. Terakura, and S. Blügel, Phys. Rev. B **44**, 3459 (1991).
- <sup>17</sup> K. Kobayashi, Y. Morikawa, K. Terakura, and S. Blügel, Phys. Rev. B **45**, 3469 (1992).
- <sup>18</sup> B. L. Zhang, C. T. Chan, and K. M. Ho, Phys. Rev. B **44**, 8210 (1991).
- <sup>19</sup> P. S. Mangat, P. Soukiassian, K. M. Schirm, L. Spiess, S. P. Tang, A. J. Freeman, Z. Hurych, and B. Delly, Phys. Rev. B **47**, 16 311 (1993).
- <sup>20</sup> A. J. Smith, W. R. Graham, and E. W. Plummer, Surf. Sci. Lett. **243**, L37 (1991).
- <sup>21</sup> R. E. Schlier and H. E. Farnsworth, J. Chem. Phys. **30**, 917 (1959).
- <sup>22</sup> D. J. Chadi, Phys. Rev. Lett. **43**, 43 (1979).
- <sup>23</sup> R. M. Tromp, R. J. Hamers, and J. E. Demuth, Phys. Rev. Lett. **55**, 1303 (1985).
- <sup>24</sup> R. A. Wolkow, Phys. Rev. Lett. **68**, 2636 (1992).
- <sup>25</sup> J. Dąbrowski and M. Scheffler, Appl. Surf. Sci. **56**, 15 (1992).
- <sup>26</sup> G. Jayarm, P. Xu, and L. D. Marks, Phys. Rev. Lett. **71**, 3489 (1993).
- <sup>27</sup> H. Wang, R. Lin, and X. Wang, Phys. Rev. B **36**, 7712 (1987).
- <sup>28</sup> Y. Enta, S. Suzuki, and S. Kono, Phys. Rev. Lett. **65**, 2704 (1990).
- <sup>29</sup> T. Tabara, T. Aruga, and Y. Murata, Surf. Sci. **179**, L63 (1987); M. Kubota and Y. Murata, Phys. Rev. B **49**, 4810 (1994).
- <sup>30</sup> Z. Zhu, N. Shima, and M. Tsukada, Phys. Rev. B **40**, 11 868 (1989).
- <sup>31</sup> P. Hohenberg and W. Kohn, Phys. Rev. **136**, B864 (1964); W. Kohn and L. J. Sham, *ibid.* **140**, A1133 (1965).
- <sup>32</sup> E. Wigner, Trans. Faraday Soc. **34**, 678 (1938).
- <sup>33</sup> N. Troullier and J. L. Martins, Solid State Commun. **74**, 613 (1990); Phys. Rev. B **43**, 1993 (1991); **43**, 8861 (1991).
- <sup>34</sup> L. Kleinman and D. M. Bylander, Phys. Rev. Lett. **48**, 1425 (1982).
- <sup>35</sup> S. G. Louie, S. Froyen, and M. L. Cohen, Phys. Rev. B **26**, 1738 (1982).
- <sup>36</sup> C. Kittel, *Introduction to Solid State Physics*, 6th ed. (Wiley, New York, 1986).
- <sup>37</sup> C. H. Park, I.-H. Lee, and K. J. Chang, Phys. Rev. B **47**, 15 996 (1993).
- <sup>38</sup> H. Hellmann, *Einführung in die Quantenchemie* (Deuticke, Leipzig, 1937), p. 285; R. P. Feynman, Phys. Rev. **56**, 340 (1939).
- <sup>39</sup> F. Bechstedt and D. Reichardt, Surf. Sci. **202**, 83 (1988).
- <sup>40</sup> A. García and J. E. Northrup, Phys. Rev. B **48**, 17 350 (1993).
- <sup>41</sup> J. Dąbrowski, E. Pehlke, and M. Scheffler, Phys. Rev. B **49**, 4790 (1994).
- <sup>42</sup> J. Ihm, D. H. Lee, J. D. Joannopoulos, and J. J. Xiong, Phys. Rev. Lett. **51**, 1872 (1983).
- <sup>43</sup> M. C. Payne, N. Roberts, R. J. Needs, M. Needels, and J. D. Joannopoulos, Surf. Sci. **211**, 1 (1989).
- <sup>44</sup> G. X. Qian, R. M. Martin, and D. J. Chadi, Phys. Rev. B **38**, 7649 (1988).
- <sup>45</sup> F. Reif, *Fundamentals of Statistical and Thermal Physics* (McGraw-Hill, New York, 1965).